Sensors and Actuators B 250 (2017) 412–419

Contents lists available at ScienceDirect

Sensors and Actuators B: Chemical

journal homepage: www.elsevier.com/locate/snb

Co–doped stannates /reduced graphene composites: Effect of cobalt substitution on the electrochemical sensing of hydrogen peroxide

C.J. Venegas[a,b], E. Yedinak[a,b], J.F. Marco[d], S. Bollo[b,c,*], D. Ruiz-León[a,**]

[a] Laboratorio de Fisicoquímica y Electroquímica del estado Sólido, Facultad de Química y Biología, Universidad de Santiago de Chile, Av. Libertador Bernardo O'Higgins n° 3363, Santiago, Chile
[b] Centro de Investigación de Procesos Redox (CiPRex), Facultad de Ciencias Químicas y Farmacéuticas, Universidad de Chile, Santiago, Chile
[c] Advanced Center for Chronic Diseases (ACCDiS), Facultad de Ciencias Químicas y Farmacéuticas, Universidad de Chile, Santiago, Chile
[d] Instituto de Química-Física Rocasolano, CSIC, 28006 Madrid, Spain

ARTICLE INFO

Article history:
Received 9 January 2017
Received in revised form 12 April 2017
Accepted 24 April 2017
Available online 29 April 2017

Keywords:
Cobalt stannate
Reduced graphene oxide composites
Hydrogen peroxide oxidation
Ceramic oxides
Electrochemical

ABSTRACT

Co–doped stannates, $Zn_{2-x}Co_xSnO_4$ ($0.5 \leq x \leq 1.5$), were produced by ceramic synthesis starting from the $ZnSnO_4$ phase. Morphology, structure, and composition of synthesized compounds were examined using scanning electron microscopy, X-ray diffraction analysis (XRD), and X-ray photoelectron spectroscopy (XPS). Using XPS, cobalt ions are shown to have an oxidation state of 2^+, and XRD patterns showed the same crystalline structure for all $Zn_{2-x}Co_xSnO_4$ ($0.5 \leq x \leq 1.5$) phases, i.e., they are isostructural. The morphology of synthesized compounds shows appreciable differences in particle sizes which range from 80 nm to 500 nm, depending on how the ceramic was synthesized and the cobalt concentration. Co–doped stannates /reduced graphene (rGO) composites were prepared and used to modify glassy carbon electrodes (GCE). The resulting electrodes were evaluated for the amperometric determination of hydrogen peroxide. The catalytic activity of composites towards the oxidation of hydrogen peroxide was highly dependent on quantity of cobalt in the ceramic compound, and also on the quantity of rGO present in the composite. The pure cobalt stannate phase with a ratio of 8:1 (ceramic:rGO) exhibited the best catalytic activity towards hydrogen peroxide oxidation at low potentials (0.400 V). A linear relationship between current and hydrogen peroxide concentration was obtained with a sensitivity of 0.43 $\mu A m M^{-1} cm^{-2}$ and a detection limit of 0.31 μM.

© 2017 Elsevier B.V. All rights reserved.

1. Introduction

Nowadays, the fascinating advances in materials science research and biological diagnostics have led to the rapid development of different classes of sensors for a wide range of analytes with improved sensing characteristics.

At its simplest construction, a biosensor features recognition element molecules (REM) anchored to or integrated into a solid support (the matrix) [1,2]. In general terms, a suitable matrix should enhance the signal transduction and helps to immobilize REM with retained or enhanced activity. The physico-chemical properties of the matrix directly influence the immobilization and the operational stability of the biosensor [3].

A chemical sensor is a small device that, as the result of a chemical interaction or process between the analyte and the sensor device, transforms chemical or biochemical information into an analytically useful signal [4]. Among all the chemical sensors reported in the literature, electrochemical sensors are the most attractive because of their remarkable sensitivity, experimental simplicity, and low cost. The signal from the transducer can be a current (amperometry), a voltage (potentiometry), or impedance/conductance changes (conductimetry) [5].

One of the most interesting analytes from the chemical and biological point of view is hydrogen peroxide (H_2O_2) because it plays important roles in the electron transfer process of hundreds of enzymes in biological systems [6], is present in several cleaning products, or is a by-product of several chemical reactions. However, the detection of H_2O_2 is problematic for unmodified or bare electrode surfaces, since the electrochemical oxidation of H_2O_2 takes place at high overpotentials, which results in passivation of the electrode. Therefore, H_2O_2 detection remains a challenge for electrochemical sensors.

* Corresponding author.
** Corresponding author.
E-mail addresses: sbollo@ciq.uchile.cl (S. Bollo), domingo.ruiz@usach.cl (D. Ruiz-León).

http://dx.doi.org/10.1016/j.snb.2017.04.154
0925-4005/© 2017 Elsevier B.V. All rights reserved.

The literature reports several studies that attempted to decrease the overpotential of hydrogen peroxide oxidation by chemically modifying the electrode surfaces which enhanced the analytical response, minimized surface fouling, and improved electron transfer kinetics. Several materials are reported as modifiers, such as peptide nanotubes [7] Au nanoparticle [8,9], TiO_2 nanostructured film [10], carbon structures such as graphene, fibers [11,12] and carbon nanotubes [13,14]. In this way, chemically modified electrodes (CMEs) provide one approach to the development of these analytical devices. CMEs are important constituents of both immobilized reagent systems and sensitive layers. In trace analysis, during the accumulation reaction, CMEs have improved sensitivies and selectivities because of their own electrocatalytic properties and/or their capacities to immobilize electrocatalytic reagents.

The majority of modified electrodes can be obtained by chemisorption, covalent bonding, and film deposition [15–18]. Among the wide range of electrode modifiers, inorganic materials, such as zeolites, silica-based hybrid materials, and clays, have attracted the attention of materials science researchers, in particular for their analytical applications [19–23]. The excellent electron conduction ability and chemical stability with high isoelectric point (approximately 9) makes oxides particularly attractive materials for sensor applications [24–27]. These properties can be further enhanced through the chemical functionalization of the oxide surface or doping with ions which result in interesting electrical properties. In addition, oxide films can be prepared by methods amenable to large-scale manufacturing at temperatures that allow for low-cost operation and flexible substrates [28].

Recent studies have shown that inorganic materials based on cobalt oxides, such as CoO, Co_3O_4 and cobalt phthalocyanines show electrocatalytic activity in hydrogen peroxide detection [29,30]. It is clear that the use of cobalt as an activator in such compounds is particularly important for ceramic oxides. In this context, metal stannate, M_2SnO_4, a ternary oxide spinel in the family of transparent conducting oxides, poses an interesting semiconducting material. Zn_2SnO_4 is well known to display a high sensitivity to various gases, with high intrinsic electrical resistivity, making it suitable for a wide range of applications, such as humidity sensors, transparent conducting electrodes and negative electrode for Li-ion batteries [31]. It has been successfully prepared by various methods (hydrothermal, thermal evaporation, sol-gel synthesis, and mechanochemical activation followed by solid-state reactions) [32,33]. Most important, zinc stannate is amenable to cobalt substitution in its crystalline structure.

On the other hand, integrating low quantities of carbon nanomaterials to form nanocomposites have been shown to dramatically improve a material's electrical and thermal conductivity and/or mechanical strength [34,35]. Combining the large surface area of carbon material with electrochemically active inorganic compounds that facilitate redox reactions has led to very effective CMEs. Electrodes based on carbon-inorganic composites require the inorganic component to be stable in normal operating conditions without any structural changes, have two or more oxidation states, and be conductive to both electrons and ions [36]. As an example, mesoporous Co_3O_4 nanoparticles (NPs) with specific surface area around 200 m^2/g have been synthesized and demonstrated enhanced ion transfer ability with a specific capacitance of approximately 400 F/g at 0.5 A/g. When Co_3O_4 NPs were deposited onto carbon nanotubes/graphene via chemical/hydrothermal method, the nanocomposite resulted in an overall higher specific capacitance than the Co_3O_4 NPs alone [37]. It is anticipated that the use of carbon material together with an inorganic compound will produce composites with good perspectives in the development of more efficient electrochemically active materials for the next generation of electrochemical devices

Considering all these aspects, in the present study, novel electroceramic/graphene composites based on cobalt-substituted Zn_2SnO_4 ($Zn_{2-x}Co_xSnO_4$, $0 \leq x \leq 2$) as inorganic oxide were prepared. The effect of the cobalt concentration in the electroceramic compound on the electrochemical detection of hydrogen peroxide was studied. To the best of our knowledge, this approach has not been carried out successfully so far.

2. Experimental

2.1. Reagents

All chemicals were of analytical grade. Zinc oxide (Merck, 99%), cobalt oxide (Merck, 99.9%), tin oxide (Merck, 99.9%), tin chloride pentahydrate (Merck, 98.0%), zinc chloride (Merck, 98%), sodium carbonate (Merck, 99.9%), hydrogen peroxide (Merck, 30%). Graphene oxide (GO) and reduced graphene oxide (rGO) were obtained from Graphenea®. Nafion® was purchased from Sigma Aldrich. A 0.01 M NaOH solution was used as a supporting electrolyte. All the other chemicals, such as H_2O_2, were of analytical grade and used as received. All electrochemical solutions were prepared with ultrapure water ($\rho = 18\ M\Omega\ cm$) from a Millipore-Milli-Q system.

2.2. Synthesis of ceramic compounds

Synthesis of Zn_2SnO_4

Zinc chloride ($ZnCl_2$) and tin tetrachloride ($SnCl_4{\cdot}5H_2O$) were used as the zinc and tin sources, respectively, for the hydrothermal synthesis of Zn_2SnO_4. The two sources were dissolved in distilled water to form two transparent solutions. The tin tetrachloride solution was slowly added to the zinc chloride solution. A molar ratio Zn:Sn of 2:1 was maintained throughout this work. As a mineralizer, sodium carbonate (Na_2CO_3) solution was added drop-wise to the mixture under magnetic stirring. After magnetic stirring for 15 min, the slurry was transferred into a 23-mL Teflon-lined stainless steel autoclave. The mixture was subjected to hydrothermal conditions in the temperature range of 120–230 °C for up to 30 h. After the reaction, the autoclave was naturally cooled to room temperature. The resulting precipitates were centrifuged at 3000 rpm, washed three times with distilled water and twice with ethanol successively, and dried at 60 °C in an oven for 8 h before further characterization.

Cobalt substitution in Zn_2SnO_4 structure

The method of solid state reaction is the most used in the preparation of ceramic materials and requires a stoichiometric mixture of chemicals precursors. Upon heating to mild temperatures and high pressures, the desired ceramic phase will be formed [38].

Solid solutions of $Zn_{2-x}Co_xSnO_4$ ($x = 0.5, 1.0, 1.5$) were prepared using the appropriate stoichiometric quantities according to Eq. (1). The reagents were mixed in a mortar agate, adding acetone to the paste so as to homogenize the sample.

$$(2-x)\,ZnO + SnO_2 + x\,CoO \rightarrow Zn_{2-x}Co_xSnO_4\ (0 \leq x \leq 2) \quad (1)$$

The samples were placed in an alumina crucible and calcined in an oven for 24 h at 1000 °C. After calcination, the samples were again ground in an agate mortar and calcined a second time at 1000 °C for 12 h to ensure complete homogeneity.

Synthesis Co_2SnO_4

Co_2SnO_4 synthesis was prepared according to Eq. (2), following the same procedure for the solid solutions.

$$2\ CoO + SnO_2 \rightarrow Co_2SnO_4 \quad (2)$$

2.3. Electroceramic materials characterization

The X-ray diffraction (XRD) data were collected at room temperature on an MTI EQ-MD-10-LD precision mini powder diffractometer, with CuKα radiation in the range $16 < 2\theta < 70^{\circ}$, with counting time of 1 s over the 0.1°(2θ) steps. The analysis of crystalline phases was performed using the Crystal Impact Match program with PDF-2 database. Parameter lattices were calculated using the STOE XPOW software. The surface morphology was imaged using a scanning electron microscope (SEM), TESCAN, Vega 3 model. Compositional study was conducted by analysis of energy dispersive spectroscopy (EDS) using a Bruker probe, model QUANTAX 400a series. XPS spectra were recorded with a PHOIBOS-150 (Specs) electron analyzer under a vacuum better than $1 \times 10-9$ mbar, using Mg Kα radiation (1253.6 eV) and a constant pass energy of 200 eV and 20 eV for the wide scan and narrow scan spectra, respectively. All binding energies (BE ± 0.2 eV) were charge–corrected to the C 1s signal of the adventitious contamination carbon layer, set at 284.6 eV.

2.4. Electrochemical measurements

Modification of Glassy Carbon Electrodes (GCEs) with composite material. 1 mg of rGO or GO was dispersed in 1 mL of Nafion (2% in ethanol) together with a quantity of electroceramic material by sonication for 15 min. The sonication procedure was repeated three times. Prior to surface modification, each GCE was polished with 0.3 and 0.05-μm alumina slurries for 1 min. The immobilization of composite was performed by drop casting 10 μL of the dispersion onto the GCE followed by drying the dispersion on the GCE for 15 min at 50 °C. The resulting modified electrodes were referenced as $Zn_{2-x}Co_xSnO_4$ ($0 \leq x \leq 2$)/(r)GO.

Electrochemical recordings were performed on a Palm instrument BV. A three-electrode cell was used with an Ag/AgCl, 3 M KCl (CH Instrument) and a platinum wire as reference and auxiliary electrodes, respectively. The working electrode was a glassy carbon electrode (GCE, CH. Instrument) modified with the composites.

Electrochemical detection of hydrogen peroxide by modified electrodes. Amperometric measurements were conducted by applying the desired working potential and allowing the transient currents to decay to a steady-state value prior to the addition of H_2O_2 and subsequent current monitoring. The experiments were conducted in a stirred supporting electrolyte solution, either NaOH.

3. Results

3.1. Characterization of electroceramic compounds

Fig. 1 shows that all XRD patterns of electroceramic materials have the same crystalline structure, therefore we can conclude that, regardless of cobalt content, these ceramics are isostructural and are described by the Fd3 m space group. There are no peaks corresponding to contaminants or unreacted secondary phases.

Considering the size of the divalent cationic zinc and cobalt radii – Zn^{2+} (0.74 Å) and Co^{2+} (0.78 Å) – it can be assumed that the substitution of zinc ions by cobalt ion in the structure of Zn_2SnO_4 will increase the cell size. Fig. 2 shows the slight shift in the 2Θ values as the concentration of Co in the structure increases. This is clear evidence of the incorporation of cobalt ions which does not result in a change in the crystal structure of the compound. From the XRD spectra, the cell parameters were calculated and are listed in Table 1S (Supporting information).

The morphology of synthesized compounds shows appreciable differences in particle size for each material. In the case of Zn_2SnO_4 prepared by a hydrothermal method, nanosized particles are observed (Fig. 1S-A, supporting information) with an average size of 80 nm. For the composites prepared from solid solutions, a more uniform particle size distribution is observed with typical sizes ranging between 0.30–0.38 μm. In the case of Co_2SnO_4, larger particles are observed, fluctuating between 400 and 700 nm (Fig. 1S-B, supporting information).

Table 1
Atomic percent and experimental molar ratio (Zn:Co) for solid solutions $Zn_{2-x}Co_xSnO_4$ in the range ($0 \leq x \leq 2$).

	Compositional analysis (atomic%)		
Element	$Zn_{1.5}Co_{0.5}SnO_4$	$ZnCoSnO_4$	$Zn_{0.5}Co_{1.5}SnO_4$
Co	9.70	18.75	29.88
Zn	29.39	19.02	9.92
O	45.75	47.43	44.41
Sn	15.16	14.79	15.79

The results of chemical analysis (see Table 1) state that the molar ratios Zn:Co experimentally obtained correlate well with nominal molar ratios. In general terms, is clear that the proportion of cobalt in the compound increases the particle size. In this particular case, the synthesis of Zn_2SnO_4 by the hydrothermal method exhibited the smallest particle size. The increased cobalt proportion in the crystal structure coincides with the cell parameters calculated by X-ray diffraction.

Fig. 3A shows the wide scan XPS spectra recorded from $Zn_{2-x}Co_xSnO_4$ ($0 \leq x \leq 2$) samples. The more intense photoemission lines of the elements that compose the samples are labelled. As can be observed, the qualitative composition is in agreement with the formulation of the different compounds. The quantitative atomic ratios were obtained from the narrow scan spectra corresponding to the main core levels of the different elements using the Multiquant XPS quantification software [39]. This software takes into account the existence of the adventitious carbon overlayer and the effect that this brings about on the attenuation of electrons having very different kinetic energies. The spectral areas were obtained by peak integration after subtraction of a Shirley background [39]. The results are presented in Table 2S (supporting information). In general, all the samples, with the exception of $Zn_{1.5}Co_{0.5}SnO_4$, show large oxygen concentrations. These results are not unusual in this type of material and can be related to the presence of surface organic contaminants, hydroxyl groups, or various types of physi- and chemi-sorbed water [40].

The Co 2p spectra recorded from all the samples are essentially identical. Fig. 3B shows a representative example. They are constituted by a main photoemission spin-orbit doublet characterized by the binding energies of the corresponding Co $2p_{3/2}$ and Co $2p_{1/2}$ core levels of 780.6 and 796.2 eV, respectively. They also show strong shake-up satellite structure at 786.1 and 802.1 eV. These spectral features, including the large intensity of the shake-up satellites and the binding energy values measured, are characteristic of those shown by Co^{2+} species in spinel-related compounds [41,42]. In order to determine if the spectra contained a minor contribution from Co^{3+}, we fitted them considering an additional doublet at the binding energies characteristic of this Co species [42]. However, in all cases, the quality of the fit was considerably worse than that obtained when considering only a single Co^{2+} contribution.

3.2. Composite ($Zn_{2-x}Co_xSnO_4$ ($0 \leq x \leq 2$)/rGO) modified electrode characterization

The morphology of the surface of the glassy carbon electrode modified with Co_2SnO_4, rGO, and Co_2SnO_4/rGO dispersed in 2% Nafion in ethanol, were studied by scanning electron microscopy (SEM). Fig. 4A shows a typical SEM image of Co_2SnO_4 dispersed in Nafion and drop casted onto the electrode. Average grain sizes

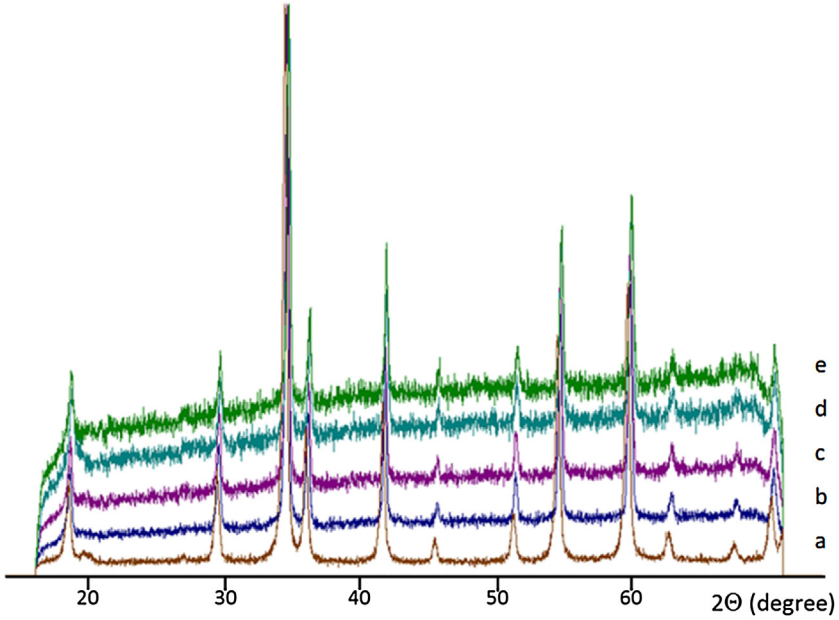

Fig. 1. Diffraction pattern of the synthesized electroceramic materials; (a) Zn_2SnO_4; (b) $Zn_{1.5}Co_{0.5}SnO_4$; (c) $ZnCoSnO_4$; (d) $Zn_{0.5}Co_{1.5}SnO_4$ and (e) Co_2SnO_4.

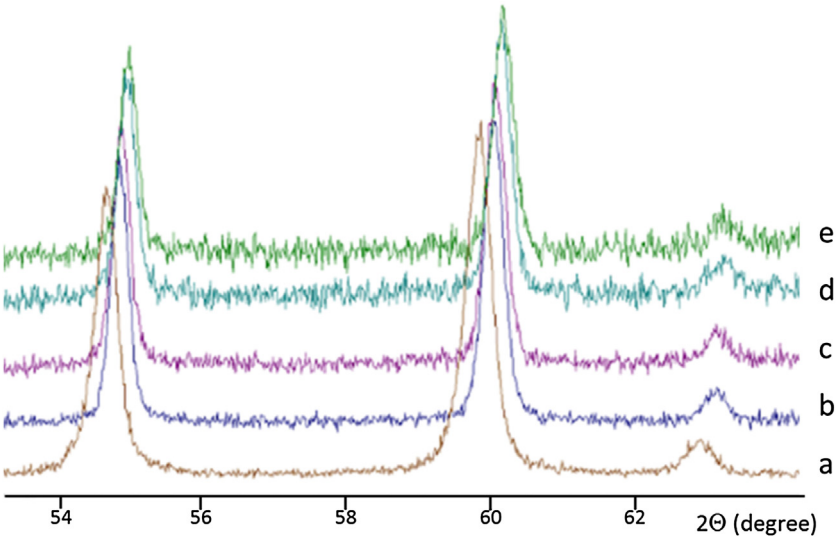

Fig. 2. XRD displacement due to Cobalt insertion. (a) Zn_2SnO_4; (b) $Zn_{1.5}Co_{0.5}SnO_4$; (c) $ZnCoSnO_4$; (d) $Zn_{0.5}Co_{1.5}SnO_4$ and (e) Co_2SnO_4.

of about 0.5 μm can be clearly seen. Comparing Fig. 4A with an SEM of Co_2SnO_4 which was not dispersed in Nafion (Fig. 1S-B), no obvious difference in the morphology, either in size or shape of the crystals, is observed. Therefore, it was concluded that sonication during the preparation of the dispersion of the electroceramic did not change their morphology significantly. Fig. 4B reveals uniform surface coverage of the graphene dispersed in Nafion and dried on the electrode. Finally, Fig. 4C shows an SEM image for the 8:1 Co_2SnO_4/rGO composite, where it is readily observed that the ceramic particles are integrated throughout the rGO/Nafion layer.

The electroactive surface areas of the [43] modified electrodes were estimated by chronoamperometry using hydroquinone as a redox probe. The results are presented in Table 2 and indicate that there are not great differences among the resulting electrodes, although by SEM images a great difference was observed for the ceramic particle sizes ranging from nanometer to almost a micron, depending on cobalt concentration. One explanation for relatively similar electroactive areas may be the use of Nafion as dispersing agent which wraps up the ceramic particle and reduced graphene oxide.

Table 2
Effective surface area of each composite-modified electrode.

Electrode[a]	area/cm^2
Zn_2SnO_4/rGO	0.014
$Zn_{1.5}Co_{0.5}SnO_4$/rGO	0.008
$ZnCoSnO_4$/rGO	0.021
$Zn_{0.5}Co_{1.5}SnO_4$/rGO	0.012
Co_2SnO_4/rGO	0.021

[a] 4:0.5 proportion.

3.3. Hydrogen peroxide electrochemical response at GC-modified electrodes

The reaction media, dispersion concentrations in Nafion, ceramic/graphene proportion in the composite, and the type of

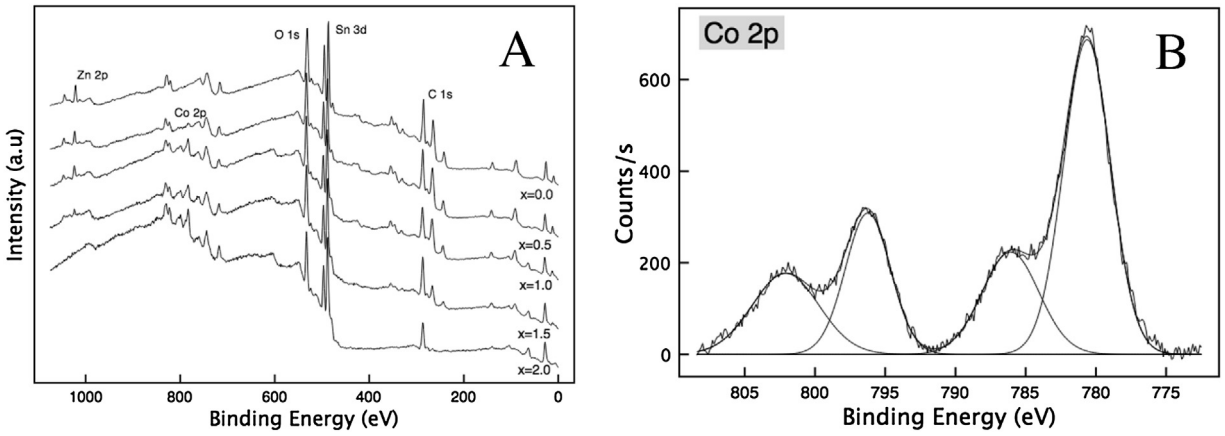

Fig. 3. (A) Wide scan XPS spectra recorded from the different $Zn_{2-x}Co_xSnO_4$ ($0 \leq x \leq 2$) samples. (B) Co 2p spectrum recorded from Co_2SnO_4.

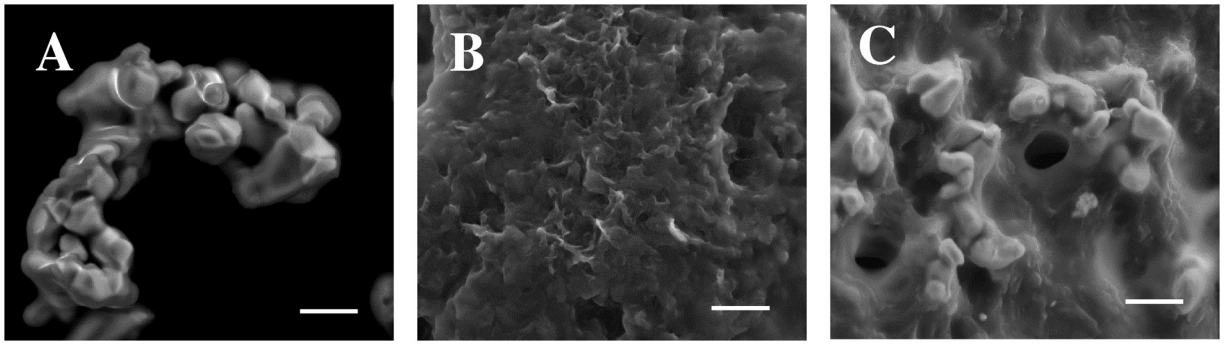

Fig. 4. SEM micrographs of GC modified electrodes with: (A) 4 mg/mL of Co_2SnO_4, (B) 0.5 mg/mL of rGO and (C) 8:1 mg/mL of Co_2SnO_4/rGO composite. Dispersing agent: Nafion® (2% in ethanol). 60.000× magnification, scale bar: 1 μm.

graphene-base material (GBM) used were optimized for hydrogen peroxide detection by amperometric recordings. The main results indicate that the best response is obtained when a solution of 0.01 M NaOH (pH 12.0) is used as supporting electrolyte. No influence on the response is observed with additions of NaCl. No significant changes in amperometric responses were detected as a result of varying the percentage of Nafion in ethanol between 0.5%–2% (data not shown).

Fig. 5A shows the amperometric recordings for successive additions of 10 μM hydrogen peroxide that were obtained from GCEs modified with dispersions of 8:1, 4:1, 2:1 and 1:1 Co_2SnO_4/rGO (amperograms a, b, c and d respectively), and rGO alone (amperogram e). Well-defined responses were obtained with a clear enhancement in the amperometric response for Co_2SnO_4/rGO (8:1). With lower concentrations of cobalt, null or small increments in the electrochemical response of hydrogen peroxide were produced in comparison with rGO alone. As the size of these ceramic particles are in the range of 500 nm and the rGO sheets are around 1 μm, it would be expected that an excess of rGO hindered the possibility of an efficient contact with the electroceramic which adversely affects the signal response. Thus, we can conclude that it is necessary to use a ratio of electroceramic to rGO that encourages good contact between the ceramic particles and the graphene sheets.

The effect of the nature of GBM (i.e., reduced graphene oxide (rGO) versus graphene oxide (GO)) on the catalytic activity towards hydrogen peroxide was evaluated (Fig. 5B). The results indicate that, independent of GBMs, a clear synergic effect is observed when both the electroceramic and GBM material are present on the electrode surface. Comparing between the GBM materials, more than 3 times the current intensity was obtained when composite is generated using rGO rather than GO.

The ratio Zn^{2+}/Co^{2+} in the ceramic was critical on the electrochemical response of modified electrodes to hydrogen peroxide. Fig. 6 compares the sensitivities obtained from amperometric recordings of hydrogen peroxide at GCE/rGO-ceramic electrodes obtained at 0.700 V using different Zn^{2+}/Co^{2+} ratio. A well-defined response is obtained after each addition of hydrogen peroxide with a positive correlation between quantity of cobalt in the ceramic material and current measured. At the pure phase with Zn^{2+} or at low concentrations of cobalt (0.5 and 1.0), no differences were observed in the electrochemical response of modified electrodes. However, when the proportion of cobalt is 1.5, an increase in the hydrogen peroxide sensitivity is observed, but it is only when cobalt is in the pure phase there is a clear increase in the sensitivity of the modified electrode. The results permit us to conclude that the best electrocatalytic response is obtained with Co_2SnO_4 and that Zn^{2+} produce a passivation of the surface. Therefore, the selected conditions to prepare the sensor were Co_2SnO_4:rGO (8:1), 2% Nafion, and of 0.01 M NaOH (pH 12.0) as electrolytic medium.

3.4. Analytical performance of Co_2SnO_4/rGO electrode

Fig. 7A shows hydrodynamic voltammograms for 10 μM hydrogen peroxide obtained at Co_2SnO_4/rGO (8:1) modified electrode. For the unmodified GCE, the oxidation of hydrogen peroxide is observed from 0.750 V onwards [33]. For the GCE modified with the 8:1 Co_2SnO_4/rGO composite, there is a decrease in the potential for the oxidation of hydrogen peroxide to 0.200 V, while the reduction is negligible even at −0.400 V. The electrocatalytic effect of the composite on the electrochemical behavior of hydrogen peroxide is

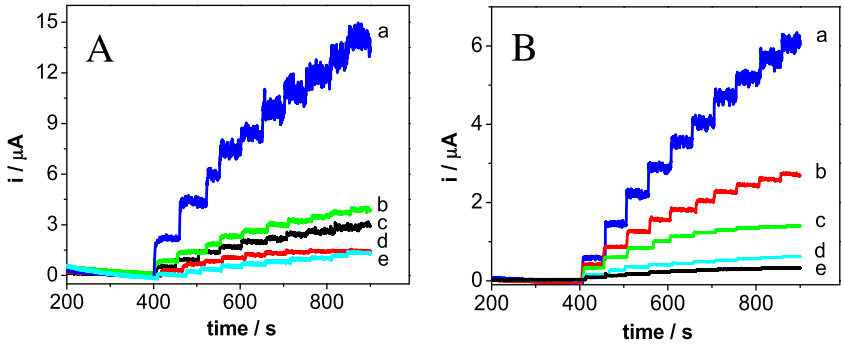

Fig. 5. Amperometric recording for successive additions of 0.05 mM hydrogen peroxide at (A) Co_2SnO_4/rGO proportions of (a) 8:1, (b) 4:1, (c) 2:1 and (d) 1:1. Amperogram (e) correspond to 0.5 mg/mL rGO alone. (B) (a) Co_2SnO_4/rGO, (c) Co_2SnO_4/GO. (b), (d) and (e) are rGO and GO and Co_2SnO_4 respectively. Co_2SnO_4/GBM proportion (8:1), Applied potential: 0.700 V. Supporting electrolyte NaOH 0.01 M. (For interpretation of the references to colour in this figure legend, the reader is referred to the web version of this article.)

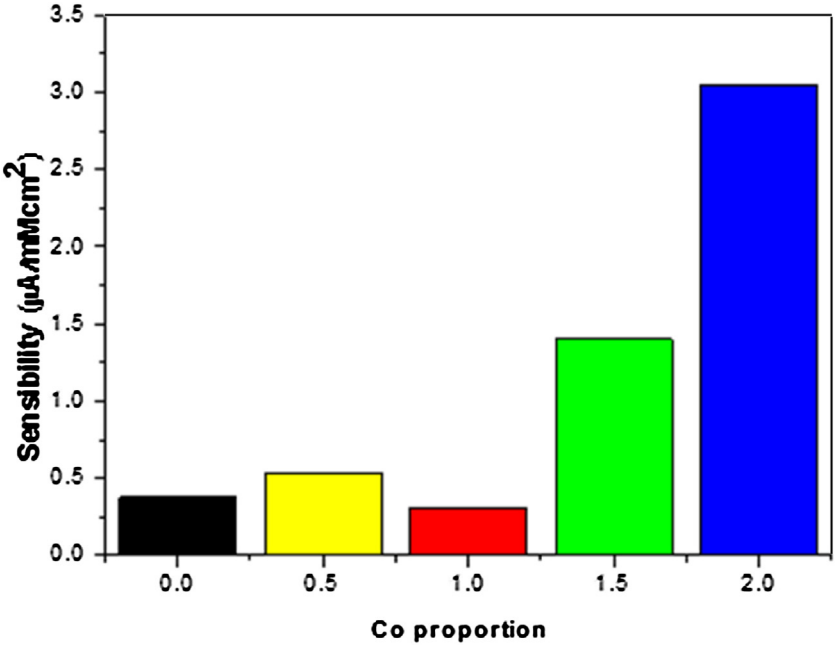

Fig. 6. Sensitivity towards hydrogen peroxide obtained from amperometric experiments at different cobalt concentrations in the electroceramic oxide. $Zn_{2-x}Co_xSnO_4$ ($0 \leq x \leq 2$)/OGr electrodes (8:1), applied potential: 0.400 V. Supporting electrolyte NaOH 0.01 M.

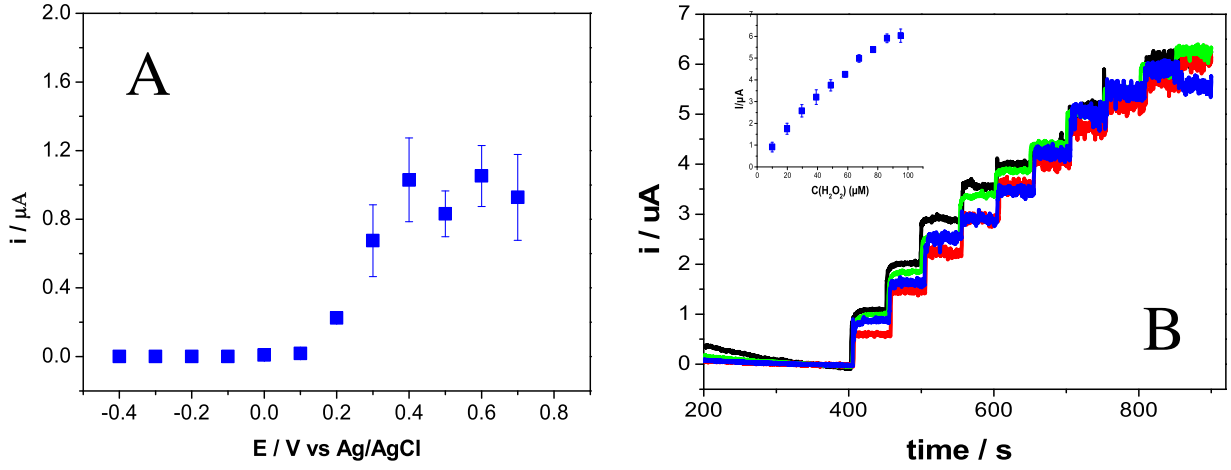

Fig. 7. (A) Hydrodynamic voltammograms for 0.050 M hydrogen peroxide at Co_2SnO_4/rGO 8:1 electrode. (B) Amperometric recording of 4 independent electrodes at 0.400 V. Inset: Calibration plot. Supporting electrolyte NaOH 0.01 M.

Table 3
Comparison of various sensors for the determination of H_2O_2.

Electrode	Electrolyte	Potential (V)	Sensitivity ($\mu A\,mM^{-1}\,cm^{-2}$)	LOD (μM)	ref
Co_3O_4 nanoparticles	NaH_2PO_4-NaOH (pH 10)	−0.70	–	4.40	[44]
MnO_2/GO nanocomposite	0.1 M NaOH	−0.30	38.20	0.80	[45]
CoOOH nanolamines	0.1 M NaOH	0.10	99.00	40.00	[46]
Ftalocianine Co(II) – Porfirine Co(II)	Buffer Fosfato (pH = 10)	0.55	0.45	6.00	[47]
CuO Nanoflowers	Buffer Fosfato (pH = 7)	−0.3	0.32	8.00	[48]
Co_2SnO_4/rGO	0.01 M NaOH (pH = 12)	0.40	0.43	0.31	This work

clear, and can even be observed using composites containing lower quantities of cobalt (not shown). The selected potential to develop the analytical method was 0.400 V because at this potential, the maximum current was observed. Fig. 7B shows the amperometric recordings obtained at 0.400 V for successive additions of 10 μM hydrogen peroxide using four different electrodes. The calibration plot (Inset Fig. 7B) shows a linear range between 10 and 80 μM hydrogen peroxide, with a sensitivity of $(0.064 \pm 0.002)\ \mu A\,mM^{-1}$ ($r^2 = 0.9998$) or $0.430 \pm 0.012\ \mu A\,mM^{-1}\,cm^{-2}$ and a detection limit of 0.31 μM (taken as $3.3\,\sigma/S$ where σ is the standard deviation of the blank signal and S the sensitivity) and a quantification limit of 0.93 μM (taken as $10\,\sigma/S$ where σ is the standard deviation of the blank signal and S the sensitivity). The Co_2SnO_4/rGO (8:1) modified electrode revealed a high reproducibility, with a relative standard deviation of 3.1% calculated from the sensitivities for hydrogen peroxide obtained with four different sensors.

Table 3 shows a comparison of the analytical performance of our modified electrode against those reported for modified electrodes with cobalt or graphene composites on GCEs. Comparing the results, our system offers the lowest detection limit and the potential applied to detect hydrogen peroxide is lower compared with other systems [44–48]. The Co_2SnO_4/rGO (8:1) modified electrode was tested successfully to determine hydrogen peroxide content in spiked samples (commercial gargles samples) with mean recoveries between 95% and 105%.

4. Conclusions

This work reports for the first time an amperometric non-enzymatic sensor based on the excellent catalytic activity of cobalt-doped stannates/rGO composites towards the oxidation of hydrogen peroxide. The catalytic activity of composites was highly dependent on quantity of cobalt in the ceramic compound, and also of the proportion of rGO present. Compared to other cobalt modified electrodes, our sensor presents several advantages including wider dynamic linear range, excellent sensitivity, and low detection limits without need of redox mediators and represents a highly promising alternative for further developments of (bio) sensors.

Acknowledgments

Financial support from Fondecyt-CHILE (Grant 1161225) and MINECO (Spain) under project MAT2015-64110-C2-1-P are gratefully acknowledged. C.J.V acknowledges the CONICYT scholarship for Ph.D. studies in Chile and E.Y. to Fulbright Program grant sponsored by the Bureau of Educational and Cultural Affairs of the United States Department of State and administered by the Institute of International Education.

Appendix A. Supplementary data

Supplementary data associated with this article can be found, in the online version, at http://dx.doi.org/10.1016/j.snb.2017.04.154.

References

[1] S.K. Arya, S. Saha, J.E. Ramirez-Vick, V. Gupta, S. Bhansali, S.P. Singh, Recent advances in ZnO nanostructures and thin films for biosensor applications: review, Anal. Chim. Acta 737 (2012) 1–21.
[2] M. Frasconi, G. Favero, M. Di Fusco, F. Mazzei, Polyazetidine-based immobilization of redox proteins for electron-transfer-based biosensors, Biosens. Bioelectron. 24 (2009) 1424–1430.
[3] V. Gupta, ZnO based third generation biosensor, Thin Solid Films 519 (2010) 1141–1144.
[4] J.R. Stetter, W.R. Penrose, S. Yao, Chemical sensors, electrochemical sensors, and ECS, J. Electrochem. Soc. 150 (2003) S11–S16.
[5] S. Borgmann, A. Schulte, S. Neugebauer, W. Schuhmann, Amperometric biosensors, Adv. Electrochem. Sci. Eng. 2 (2011).
[6] J.D. Newman, A.P.F. Turner, Home blood glucose biosensors: a commercial perspective, Biosens. Bioelectron. 20 (2005) 2435–2453.
[7] M. Yemini, M. Reches, E. Gazit, J. Rishpon, Peptide nanotube-modified electrodes for enzyme biosensor applications, Anal. Chem. 77 (2005) 5155–5159.
[8] L. Adler-Abramovich, M. Badihi-Mossberg, E. Gazit, J. Rishpon, Characterization of peptide-nanostructure-modified electrodes and their application for ultrasensitive environmental monitoring, Small 6 (2010) 825–831.
[9] A.K. Das, C.R. Raj, Facile growth of flower-like Au nanocrystals and electroanalysis of biomolecules, J. Electroanal. Chem. 638 (2010) 189–194.
[10] A. Curulli, F. Valentini, G. Padeletti, M. Viticoli, D. Caschera, G. Palleschi, Smart (nano) materials: TiO2 nanostructured films to modify electrodes for assembling of new electrochemical probes, Sens. Actuators B Chem. 111–112 (2005) 441–449.
[11] C. Shan, H. Yang, D. Han, Q. Zhang, A. Ivaska, L. Niu, Electrochemical determination of NADH and ethanol based on ionic liquid-functionalized graphene, Biosens. Bioelectron. 25 (2010) 1504–1508.
[12] Y. Wu, X. Mao, X. Cui, L. Zhu, Electroanalytical application of graphite nanofibers paste electrode, Sens. Actuators B Chem. 145 (2010) 749–755.
[13] R.R. Moore, C.E. Banks, R.G. Compton, Basal plane pyrolytic graphite modified electrodes: comparison of carbon nanotubes and graphite powder as electrocatalysts basal plane pyrolytic graphite modified electrodes: comparison of carbon nanotubes and graphite powder as electrocatalysts, Anal. Chem. 76 (2004) 2677–2682.
[14] M. Zhang, W. Gorski, Electrochemical sensing based on redox mediation at carbon nanotubes, Anal. Chem. 77 (2005) 3960–3965.
[15] R.W. Murray, Molecular Design of Electrode Surfaces Techniques in Chemistry, vol 22, Wiley, New York, 1992, pp. 1–48.
[16] M. Ghasemi, W.R.W. Daud, S.H.a. Hassan, S.-E. Oh, M. Ismail, M. Rahimnejad, et al., Nano-structured carbon as electrode material in microbial fuel cells: a comprehensive review, J. Alloys Compd. 580 (2013) 245–255.
[17] L. Yang, Q. Zhou, G. Wang, Y. Yang, Acetylcholinesterase biosensor based on SnO2 nanoparticles-carboxylic graphene-nafion modified electrode for detection of pesticides, Biosens. Bioelectron. 49 (2013) 25–31.
[18] B.R. Braeckman, F. Boydens, D. Depla, D. Poelman, Reactive sputter deposition of Al doped TiOx thin films using titanium targets with aluminium inserts, J. Alloys Compd. 578 (2013) 44–49.
[19] S.K. Kirdeciler, E. Soy, S. Öztürk, I. Kucherenko, O. Soldatkin, S. Dzyadevych, et al., A novel urea conductometric biosensor based on zeolite immobilized urease, Talanta 85 (2011) 1435–1441.
[20] Y. Xie, H. Liu, N. Hu, Layer-by-layer films of hemoglobin or myoglobin assembled with zeolite particles: electrochemistry and electrocatalysis, Bioelectrochemistry 70 (2007) 311–319.
[21] K. Sahner, D. Schönauer, P. Kuchinke, R. Moos, Zeolite cover layer for selectivity enhancement of p-type semiconducting hydrocarbon sensors, Sens. Actuators B Chem. 133 (2008) 502–508.
[22] A. Walcarius, Electrochemical applications of silica-based organic-inorganic hybrid materials, Chem. Mater. 13 (2001) 3351–3372.
[23] A. Walcarius, Â. Lefevre, J. Rapin, G. Renaudin, M. Francois, Â.I. Nancy, Voltammetric detection of iodide after accumulation by Friedel's salt, Electroanalysis (2001) 313–320.
[24] H. Teymourian, A. Salimi, S. Khezrian, Fe_3O_4 magnetic nanoparticles/reduced graphene oxide nanosheets as a novel electrochemical and bioeletrochemical sensing platform, Biosens. Bioelectron. 49 (2013) 1–8.
[25] X. Xu, J. Qian, S. Liu, Electrochemically driven biocatalysis of the oxygenase domain of neuronal nitric oxide synthase in indium tin oxide

nanoparticles/polyvinyl alcohol nanocomposite, Bioelectrochemistry 94 (2013) 7–12.
[26] L. Yang, Q. Zhou, G. Wang, Y. Yang, Acetylcholinesterase biosensor based on SnO2 nanoparticles-carboxylic graphene-nafion modified electrode for detection of pesticides, Biosens. Bioelectron. 49 (2013) 25–31.
[27] M.H. Lee, J.L. Thomas, Y.L. Chen, C.F. Lin, H.H. Tsai, Y.Z. Juang, et al., Optical sensing of urinary melatonin with molecularly imprinted poly(ethylene-co-vinyl alcohol) coated zinc oxide nanorod arrays, Biosens. Bioelectron. 47 (2013) 56–61.
[28] J.W. Rhim, L.F. Wang, S.I. Hong, Preparation and characterization of agar/silver nanoparticles composite films with antimicrobial activity, Food Hydrocoll. 33 (2013) 327–335.
[29] M.J. Song, S.W. Hwang, D. Whang, Non-enzymatic electrochemical CuO nanoflowers sensor for hydrogen peroxide detection, Talanta 80 (2010) 1648–1652.
[30] H. Wang, Y. Bu, W. Dai, K. Li, H. Wang, X. Zuo, Well-dispersed cobalt phthalocyanine nanorods on graphene for the electrochemical detection of hydrogen peroxide and glucose sensing, Sens. Actuators B Chem. 216 (2015) 298–306.
[31] L. Qin, S. Liang, A. Pan, X. Tan, Zn_2SnO_4/carbon nanotubes composite with enhanced electrochemical performance as anode materials for lithium-ion batteries, Mater. Lett. 164 (2016) 44–47.
[32] L. Qin, S. Liang, A. Pan, X. Tan, Facile solvothermal synthesis of Zn_2SnO_4 nanoparticles as anode materials for lithium-ion batteries, Mater. Lett. 141 (2015) 255–258.
[33] Q. Zhao, X. Deng, M. Ding, J. Huang, D. Ju, X. Xu, Synthesis of hollow cubic Zn_2SnO_4 sub-microstructures with enhanced photocatalytic performance, J. Alloys Compd. 671 (2016) 328–333.
[34] X. Huang, X. Qi, F. Boey, H. Zhang, Graphene-based composites, Chem. Soc. Rev. 41 (2012) 666–686.
[35] H. Kim, A. a. Abdala, C.W. MacOsko, Graphene/polymer nanocomposites, Macromolecules 43 (2010) 6515–6530.
[36] S. Bai, X. Shen, Graphene-inorganic nanocomposites, RSC Adv. 2 (2012) 64.
[37] S. Liu, S. Sun, X.-Z. You, Inorganic nanostructured materials for high performance electrochemical supercapacitors, Nanoscale 6 (2014) 2037–2045.
[38] M. Mohai, XPS MultiQuant: multimodel XPS quantification software, Surf. Interface Anal. 36 (2004) 828–832.
[39] D.A. Shirley, High-resolution X-ray photoemission spectrum of the valence bands of gold, Phys. Rev. 135 (1972) 4709–4714.
[40] J.F. Marco, J.R. Gancedo, M. Gracia, J.L. Gautier, E. Ríos, F.J. Berry, Characterization of the nickel cobaltite, NiCo2O4 prepared by several methods: an XRD, XANES, EXAFS, and XPS study, J. Solid State Chem. 153 (2000) 74–81.
[41] J.F. Marco, J.R. Gancedo, J. Ortiz, J.L. Gautier, Characterization of the spinel-related oxides $Ni_xCo_{3-x}O_4$ (x = 0.3; 1.3; 1.8) prepared by spray pyrolysis at 350 °C, Appl. Surf. Sci. 227 (2004) 175–186.
[42] J.L. Gautier, E. Rios, M. Gracia, J.F. Marco, J.R. Gancedo, Characterisation by X-ray photoelectron spectroscopy of thin Mn_x $Ni_xCo_{3-x}O_4$ ($1 \geq x \geq 0$) spinel films prepared by low-temperature spray pyrolysis, Thin Solid Films 311 (1997) 51–57.
[43] R.N. Adams, Electrochemistry at Solid Electrodes, Marcel Decker, New York, 1969, pp. 219.
[44] J. Mu, L. Zhang, M. Zhao, Y. Wang, Co_3O_4 nanoparticles as an efficient catalase mimic: properties, mechanism and its electrocatalytic sensing application for hydrogen peroxide, J. Mol. Catal. A: Chem. 378 (2013) 30–37.
[45] L. Li, Z. Du, A novel non-enzymatic hydrogen peroxide sensor based on MnO2/graphene oxide nano composite, Talanta 82 (2010) 1637–1641.
[46] K. Lee, P. Loh, C. Sow, CoOOH nanosheet electrodes: simple fabrication for sensitive electrochemical sensing of hidrogen peroxide and hydrazine, Biosens. Bioelectron. 39 (2013) 255–260.
[47] K. Ozoemena, Z. Zhao, Immobilized cobalt(II) phthalocyanine – cobalt(II) porphyrin pentamer at a glassy carbon electrode: applications to efficient amperometric sensing of hydrogen peroxide in neutral and basic media, Electrochem. Commun. 7 (2005) 679–684.
[48] M. Song, S. Woo, D. Whang, Non-enzymatic electrochemical CuO nanoflowers sensor for hydrogen peroxide detection, Talanta 80 (2010) 1648–1652.

Biographies

Constanza J. Venegas obtained her Bachelor in Chemistry from the Universidad de Santiago de Chile in 2014. She is pursuing her PhD (Chemistry) under the supervision of Profs. Bollo and Ruiz-León at University of Chile. Her thesis title is "Development of hybrid materials based on graphene and cobalt oxide for the electrochemical detection of biomolecules".

Emily M. Yedinak obtained two Bachelors degrees in Chemical Engineering and Chemistry from Rose-Hulman Institute of Technology in 2013. Following graduation, she won a Fulbright grant to conduct a research project under the supervision of Dr. Domingo Ruiz-León and Dr. Soledad Bollo at the Universidad de Santiago de Chile and Universidad de Chile. She is now currently pursuing a PhD in Materials Science and Nanoengineering at Rice University in Houston, TX under the supervision of Dr. Matteo Pasquali and Dr. Jun Lou. Her thesis is studying single-walled carbon nanotubes for electrically conducting fibers.

José F. Marco obtained a Physics degree at the Facultad de Ciencias of Universidad de Zaragoza (Spain) in 1984 and his PhD in Physics on the atmospheric corrosion of weathering steels in the Instituto de Química-Física "Rocasolano" CSIC (Madrid Spain) under the supervision of Prof. J.R. Gancedo in 1989. He did postdoctoral positions with Dr. W. Meisel at the Institut für Anorganische und Analytische Chemie in Mainz University and with Prof. F.J. Berry at the Chemistry Department of the University of Birmingham (UK) At present, he is Senior Researcher at Instituto de Química-Física "Rocasolano" CSIC (Madrid Spain). His research interest focus on spectroscopic work in different areas where Physics, Chemistry and Materials Science merge together. He has over 180 peer-reviewed papers.

Soledad Bollo obtained her Ph. D. in Chemistry (1998) from University of Chile (Santiago, Chile). She did the postdoctoral training at New Mexico State University, Las Cruces (USA) in 1998. At present, she is Full Professor at University of Chile. Since 2013 Dr. Bollo heads the School of Pharmacy at the Faculty of Chemical and Pharmaceutical Sciences. Her research interests focus on the design and characterization of electrochemical (bio) sensors based on carbon nanomaterialss and the study of DNA damage. She has over 75 peer-reviewed papers and two book chapters.

Domingo Ruiz-León obtained his Ph. D. in Chemistry (2003) at the University of Chile (Santiago, Chile). He did the postdoctoral Fellowship at the University of Sheffield, (UK) in 2007. At present, He is Assistant Professor at University of Santiago. Since 2016 Dr. Ruiz-León heads the Chemistry Career at the Faculty of Chemistry and Biology. His research interests focus on the synthesis and characterization of electroceramic materials for energy related applications (lithium batteries, fuel cells). He has over 20 peer-reviewed papers.